

United States  
Department of  
Agriculture

Natural Resources  
Conservation  
Service

11 Campus Boulevard  
Suite 200  
Newtown Square, PA 19073

**Subject:** Soil – Ground-Penetrating Radar (GPR) Field Assistance

**Date:** 30 August 2000

**To:** Philip J. Nelson  
State Conservationist  
USDA-NRCS  
P.O. Box 11350  
Salt Lake City, Utah 84147-0350

**Purpose:**

The purpose of this investigation was to evaluate the feasibility of using GPR to determine the depth to bedrock within the Grand Staircase-Escalante National Monument.

**Participants:**

Erin Bell, Soil Scientist Trainee, USDA-NRCS, North Logan, UT  
Janis Boettinger, Assoc. Professor, Utah State Univ., Logan, UT  
Jim Doolittle, Research Soil Scientist, USDA-NRCS, Newtown Square, PA  
Marietta Eaton, Assistant Monument Manager, USDI-BLM, Kanab, UT  
Suzann Kienast, Soil Scientist, USDA-NRCS, Logan, UT  
Victor Parslow, Soil Scientist, USDA-NRCS, Richfield, UT  
Lars, Rasmussen, Range Conservationist, USDA-NRCS, Filmore, UT  
Leland Sasser, Soil Scientist, USDA-NRCS, Price, UT  
Kent Sutcliffe, Soil Scientist, USDA-NRCS, Cedar City, UT

**Activities:**

All activities were completed during the period of 31 July to 4 August 2000.

**Summary of Findings:**

1. Within Grand Staircase-Escalante National Monument, GPR is well suited to mapping the depth to bedrock in areas of coarse-textured soils that are underlain by Navajo sandstone. In these areas, GPR provides a fast, accurate, and comprehensive method for mapping bedrock depths. Compared with traditional soil survey techniques, GPR can provide greater amounts of information on the depth to bedrock and soil map unit composition (based on soil depth criteria) in shorter periods of time and with less effort.
2. At twenty-three observation points, the two-way radar pulse travel time was compared to the observed depth to subsurface interfaces that were measured with a soil auger. A very strong positive correlation ( $r = 0.999$ ) was found between the two-way travel times of the radar pulse and the measured depths to subsurface interfaces. The difference between the measured and the predicted depth to known and detected subsurface features was about 0.10 m with a range of -0.45 to 0.23 m. Based on these relationships and values, it is apparent that GPR can provide reasonably accurate measurements of the depth to bedrock in areas of coarse-textured soils that are underlain by Navajo sandstone.
3. During this investigation sixty-nine traverses were completed at nine widely spaced sites within the Grand Staircase-Escalante National Monument. Depths to bedrock interpretations were made at 676 observation points. Based on soil depth criteria, bedrock depths were shallow (0.0 to 0.5 m) at 15 percent, moderately deep (0.5 to 1.0 m) at 32 percent, deep (1.0 to 1.5 m) at 22 percent, and very deep (> 1.5 m) at 31 percent of these observation points.
4. With additional fieldwork, GPR may provide information not only on the depth to bedrock, but the nature of the contact (lithic or paralithic).

It was my pleasure to work with members of your find staff in Utah.

With kind regards,

  
James A. Doolittle  
Research Soil Scientist

cc:  
B. Ahrens, Director, USDA-NRCS, National Soil Survey Center, Federal Building, Room 152, 100 Centennial Mall North, Lincoln, NE 68508-3866  
J. Boettinger, Associate Professor, Dept. of Plants, Soils, and Biometeorology, Utah State University, Logan, Utah 84322-4820  
W. Broderson, State Soil Scientist, USDA-NRCS, PO Box 11350, Salt Lake City, UT 84147-0350  
H. Dye, MLRA Office Leader, USDA-NRCS, 3003 N. Central Suite 800, Phoenix, AZ 85012-2945  
C. Olson, National Leader, Soil Investigation Staff, USDA-NRCS, National Soil Survey Center, Federal Building, Room 152, 100 Centennial Mall North, Lincoln, NE 68508-3866  
H. Smith, Director of Soils Survey Division, USDA-NRCS, Room 4250 South Building, 14th & Independence Ave. SW, Washington, DC 20250  
K. Sutcliffe, Soil Scientist, USDA-NRCS, 2390 West Highway 56 #14, Cedar City, Utah 84720

### **Background:**

Soil scientists have been tasked with mapping Grand Staircase-Escalante National Monument. They have experienced difficulty mapping sandy soil that are greater than 100 cm to bedrock and establishing soil depth/plant relationships with traditional soil survey tools. Soil scientists use shovels and augers to acquire information on the depth to bedrock. These tools are rather slow and tedious to operate, and the data collected are therefore relatively expensive and limited. In many areas, the depth to bedrock is highly variable over short distances and extrapolations made from a limited number of widely spaced auger observations can be flawed. A large number of borings is required to adequately characterize the distribution of bedrock depths within soil map units. In addition, soils containing rock fragments limit the effectiveness of shovels and augers for measuring the depths to bedrock. In these soils, the probability of encountering a rock fragment increases with increasing soil depth. Studies have shown that the depths to bedrock are underestimated with traditional soil survey tools (Doolittle et al., 1988; Collins et al., 1989). Limited by the tools normally used, soil scientists must infer the depth to bedrock from vegetative cover and landscape position. These inferences are often based on anticipated rather than confirmed depths to bedrock. For these reasons, alternative techniques are needed to complement traditional soil survey tools, and to improve and expedite the characterization of bedrock depths within soil map units.

Alternative field methods are available. Where terrain conditions are suitable, GPR can provide high-resolution mapping of the depths to bedrock (Davis and Annan, 1989; Morey, 1974; Olson and Doolittle, 1985; Schellentrager and Doolittle, 1991). Collins and others (1989) found GPR to be more rapid, economical, and reliable than conventional auger techniques for determining the depth to bedrock and the composition of soil map units based on soil-depth criteria. Ground-penetrating radar has been used to investigate soil-bedrock relations on glacial-scoured uplands (Doolittle et al., 1988; Collins et al., 1989) and on karst (Collins et al., 1990 and 1994; Puckett et al., 1990). In areas where the underlying lithologies have strongly contrasting electrical properties or internal structure, GPR has been used to identify and characterize changes in rock types (Benson and Yuhr, 1992; Bjelm et al., 1983; Robillard et al., 1994; Sigurdsson, 1994). In addition, GPR has been used to detect low-dipping fractures or dikes in bedrock (Davis and Annan, 1989; Holloway and Mugford, 1990; Stevens et al., 1995). Typically, fracture zones have higher moisture and clay contents than the surrounding rock mass and produce strong radar reflections.

Ground-penetrating radar has also been used to differentiate weathered from unweathered rock. Robillard and others (1994) observed that the surface of unweathered bedrock often appears as a continuous reflector of variable amplitude. These researchers related variations in the amplitude of the reflected signal to differences in rock hardness and mineralogy. Leggo and others (1992) used GPR techniques to distinguish variations in the degree of argillization in granitic bedrock. Robillard and others (1994) observed corestones within more highly weathered bedrock matrix.

Recently, Jol and others (2000) and Junck and Jol (2000) used high frequency (225 to 900 MHz) antennas to study the internal stratigraphy of Navajo sandstone within Zion National Park, Utah. In these studies the quartz sandstone proved very resistive and ideal for GPR. Both inclined dune bedsets and nearly horizontal erosional surfaces were identified in these studies.

Ground-penetrating radar is not suitable for use on all soils (Doolittle, 1987) or rock types (Rubin and Fowler, 1978). Earthen materials having high electrical conductivity rapidly attenuate radar energy, restrict penetration depths, and severely limit the effectiveness of GPR. The principal factors influencing the electrical conductivity of soils and rocks are: amount and type of salts in solution, amount and type of clay, porosity, and degree of water saturation. In general, soluble salts are more thoroughly leached from soils in humid than in arid or semiarid regions. In semi-arid and arid regions, soluble salts of potassium and sodium and less soluble carbonates of calcium and magnesium are more likely to accumulate in the upper parts of the soil. These salts produce high attenuation losses that restricts the radar's penetration depth (Doolittle and Collins, 1995). The penetration depth of GPR increases as the clay content of soils decreases. Daniels and others (1988) observed a reduction in penetration depth from 5 m (with 1 GHz antenna) in sandy soils to 2 m (with a 100 MHz antenna) in clayey soils. Soils that average less than 18 percent clay are generally considered favorable to GPR. Because of high soluble salt and clay contents, the use of GPR by USDA-NRCS has been very limited in western states. However, limited areas exist in each western state where soil conditions are optimal for the use of GPR.

Extensive areas of noncalcareous, sandy soils overlying sandstone occur in Grand Staircase-Escalante National Monument. These areas are considered favorable for the use of GPR. The purpose of this investigation was to evaluate the suitability of GPR for determining the depth to bedrock, the composition of soil map units based on soil-depth criteria, and soil/plant relationships in these areas.

### **Equipment:**

The radar unit is the Subsurface Interface Radar (SIR) System-2000, manufactured by Geophysical Survey Systems, Inc.<sup>1</sup> Morey (1974), Doolittle (1987), and Daniels (1996) have discussed the use and operation of GPR. The SIR System-2000 consists of a

<sup>1</sup> Trade names are used to provide specific information. Their mention does not constitute endorsement by USDA-NRCS.

digital control unit (DC-2) with keypad, VGA video screen, and connector panel. A 12-volt battery powers the system. This unit is backpack portable and, with an antenna, requires two people to operate. A 400 MHz antenna was used in this study. The scanning time was of 60 nanoseconds (ns). Hard copies of the radar data were printed on a model T-104 printer.

The location of each GPR traverse was obtained with Rockwell Precision Lightweight GPS Receivers (PLGR).<sup>1</sup> The receiver was operated in the continuous and the mixed satellite modes. The Universal Transverse Mercator (UTM) coordinate system was used. Horizontal datum was the North American 1927. Horizontal units were expressed in meters.

#### Study Sites:

Radar traverses were conducted in the southwest portion of the Grand Staircase-Escalante National Monument in areas that are underlain by Navajo sandstone. The Navajo sandstone formed from windblown sediments that were deposited in the Jurassic and Triassic periods. Soils formed from the Navajo sandstone are noncalcareous Quartzipsamments and Torripsamments. These soils are fairly extensive (250,000 acres) within the Monument. A soil survey that included the Grand Staircase-Escalante National Monument was mapped at a scale of 1:63,360. Soil mapping units within the present boundaries of the Monument were mapped as variants of the Mespun series. Mespun soils consists of very deep, excessively drained rapidly permeable soils that formed in eolian deposits derived mainly from sandstone. Mespun is a member of the siliceous, mesic Ustic Torripsamments family.

Areas surveyed with GPR during this investigation have not been recently mapped. The study area has an upland, aridic-ustic regime. While new soils are recognized, they have not been formally established. These soils are predominantly members of either the coated, mesic, Lithic Quartzipsamments, or the coated, mesic, Ustic Quartzipsamments family. Soils are underlain by weakly cemented (paralithic materials) to strongly cemented or indurated sandstone. Depths to lithic and paralithic contacts are highly variable. Soil depths are acknowledged to be mostly moderately deep, deep, and very deep.

#### Field Procedures:

Sixty-nine GPR traverses of variable lengths were completed at nine sites. Radar surveys were completed by pulling the 400 MHz antenna along these traverse lines. As the radar antenna was pulled across the landscape, observation marks were inserted on the radar profile at intervals that ranged from about 10 to 20 paces. The site, traverse and file numbers, and the locations of starting and ending points of each traverse are listed in Table 1.

The radar profiles were reviewed in the field and printed each night. The bedrock interface was identified and depth scaled at 676 observation points. All radar profiles have been stored on disc.

Soil data were obtained from 23 auger holes collected at specific points along radar traverse lines. Soil data were compared with radar reflections to scale the radar profiles and verify interpretations (see Table 2). Detail notes of the terrain and vegetation were recorded for each traverse.

#### Calibration of GPR:

Ground-penetrating radar measures the time it takes electromagnetic energy to travel from an antenna to an interface (i.e., soil horizon, bedrock surface) and back. To convert travel time to depth requires knowledge of the velocity of pulse propagation. Several methods are available to determine the velocity of propagation. These methods include use of table values, common midpoint calibration, and calibration over a target of known depth. The last method is considered the most direct and accurate method to estimate propagation velocity. The procedure involves measuring the two-way travel time to a known reflector on the radar profile and calculating the propagation velocity by the following equation (after Morey, 1974):

$$V = 2D/T \quad [1]$$

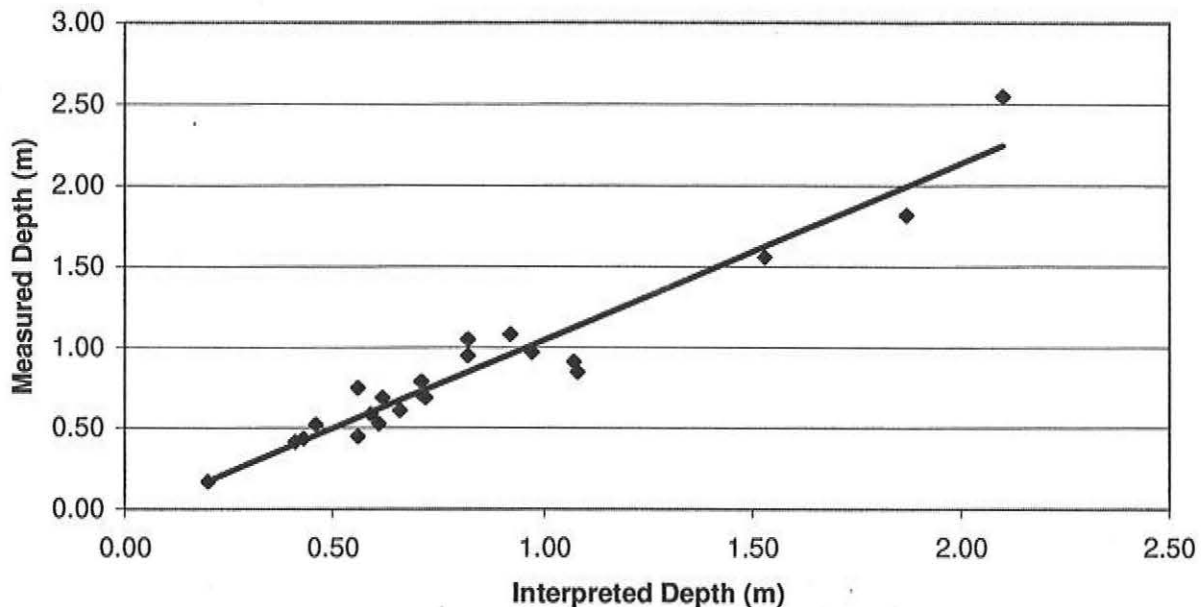
Equation [1] describes the relationship of the average propagation velocity (V) to the depth (D) and two-way pulse travel time (T) to a reflector.

At twenty-three observation points, the two-way radar pulse travel time was compared to the depth to a subsurface interface and used to estimate the average velocity of propagation. Based on the measured depths and the two-way travel times to various subsurface interfaces, and equation [1], the velocity of propagation was estimated to be about 0.1368 m/ns. A scanning time of 60 ns was used in this investigation. Using equation [1], a scanning time of 60 ns, and a propagation velocity of 0.1368 m/ns, the maximum depth of observation was estimated to be about 4.1 m.

A very strong positive relationship ( $r = 0.999$ ) was found to exist between the two-way travel times of the radar pulse and the measured depths. This relationship is shown in the Graph 1. At each of the twenty-three observation points, an interpreted depth to a known and detected subsurface reflector was determined using the average velocity of propagation (0.1368 m/ns), the two-way radar pulse travel time, and equation [1]. Using this procedure, the difference between the measured and the predicted depth to

detected subsurface features was about 0.10 m with a range of -0.45 to 0.23 m (see Table 2). Based on these relationships and values, it is apparent that GPR provides reasonably accurate depth measurements.

**Graph 1**  
**Relationship between Measured and Interpreted Depths**  
**to Subsurface Interfaces Observed on Radar Profiles**



#### Interpretations:

Figure 1 is a representative radar profile from an area that is underlain by what was interpreted to be strongly cemented or indurated sandstone. The black, vertical lines at the top of this radar profile represent equally spaced event markers or observation points. A depth scale is provided along the left-hand margin of this figure. Depths are expressed in m.

In Figure 1, the soil/bedrock contact has been highlighted with a black line. Depths to this interface range from about 1.2 to 1.8 m. In this figure, the bedrock surface provides high amplitude, relatively smooth, continuous interface that is easily identified and traced laterally. The amount of energy reflected back to an antenna by an interface separating two materials is a function of the dielectric gradient existing between the two materials. The greater or more abrupt the difference in dielectric properties, the greater the amount of energy reflected back to the antenna, and the more intense will be the amplitude of the image recorded on the radar profile. The reflection of energy from an interface is dependent upon its reflection coefficient. The reflection coefficient is expressed in the following equation (Daniels, 1996):

$$R = \sqrt{e_1} - \sqrt{e_2} / \sqrt{e_1} + \sqrt{e_2} \quad [2]$$

Where  $e_1$  and  $e_2$  are the dielectric permittivities of the two materials. The dielectric permittivity of a material is dependent upon bulk density, porosity, structure, composition, moisture content, and temperature. In Figure 1, the high amplitude of soil/bedrock interface signifies an abrupt change from loose sands to strongly cemented or indurated bedrock; a lithic contact.

The hyperbolic patterns in the upper part of Figure 1 are reflections from point objects. Point objects that occur in soils are larger tree roots, rock fragments, concretions, animal burrows, and modern cultural debris and features.

Figure 2 is a representative radar profile from an area that is underlain by what was interpreted to be weakly to moderately cemented sandstone. The black, vertical lines at the top of this radar profile represent equally spaced event markers or observation points. A depth scale is provided along the left-hand margin of this figure. Depths are expressed in m.

In Figure 2, the soil/bedrock contact is irregular, faint, and difficult to identify and trace laterally. The soil/bedrock contact has been highlighted with a black line. Depths to this interface range from about 0.9 to 1.7 m. The soil/bedrock interface has low signal amplitudes. It is inferred from the low signal amplitudes that this interface is gradual and separates less strongly contrasting materials. In Figure 2, the low amplitude of soil/bedrock interface implies a change from loose sands to weakly or moderately cemented bedrock, a paralithic contact.

The radar imagery in Figure 3 is complex. The black, vertical lines at the top of this radar profile represent equally spaced event markers or observation points. A depth scale is provided along the left-hand margin of this figure. Depths are expressed in m.

In Figure 3, the soil/bedrock contact has been highlighted with a black line. In some portions of this radar profile, this interface is indistinct and interpretations are more ambiguous. The soil/bedrock contact is spatially variable. It ranges in depth from 0.42 to 2.9 m. The recorded radar image of this interface varies in amplitudes. The varying amplitude of the soil/bedrock interface suggests lateral changes from paralithic and lithic contacts over relatively short distances. In some areas low amplitude reflections are underlain by noticeably higher amplitude reflections. The lower-lying, higher amplitude reflections are inferred to represent more contrasting (indurated?) materials. However, in other portions of Figure 3, paralithic materials may gradually grade into more strongly cemented materials with increasing soil depth and be indistinguishable. Within the underlying Navajo sandstone, steeply inclines and parallel stratifications are evident.

In the right-hand portion of Figure 3, clutter is introduced by reflections from undesired objects in the soil. Hyperbolic patterns from larger tree roots produce undesired subsurface reflections that complicate radar imagery and mask the presence of the soil/bedrock interface. In some portions of this radar profile, reflections from soil/bedrock interface are indistinguishable and interpretations are uncertain.

#### **Results:**

During this investigation sixty-nine traverses were completed at nine widely spaced sites within the Grand Staircase-Escalante National Monument. Although GPR provides a continuous record of the subsurface, interpretations were restricted to 676 observation points. At each observation point the depth to bedrock was estimated. The radar-interpreted depths to bedrock are listed in Table 3. All reported depths are in meters. In Table 3, if the depth of bedrock was greater than the depth of radar observation, the depth was recorded as 4.1 m.

Based on 676 measurements, the average depth to bedrock is 1.35 m with a range of 0 to 4.1 m (the maximum depth of radar observation in this survey). One-half the observation had interpreted depths to bedrock between 0.7 and 1.7 m. At two observation points the bedrock was exposed. Based on soil depth criteria, bedrock depths were shallow (0.0 to 0.5 m) at 15 percent, moderately deep (0.5 to 1.0 m) at 32 percent, deep (1.0 to 1.5 m) at 22 percent, and very deep (> 1.5 m) at 31 percent of the observation points.

#### **References:**

- Annan, A. P. and J. L. Davis. 1977. Radar range analysis for geologic materials. Report of Activities, Geologic Survey of Canada. Paper 77-1B. p. 117-124.
- Benson, R. and L. Yuhr. 1992. Assessment of bauxite reserves using ground penetrating radar. p. 229-236. IN: P. Hanninen and S. Autio (eds.) Fourth International Conference on Ground-Penetrating Radar. 7 to 12 June 1992. Rovaniemi, Finland. Geological Survey of Finland, Special Paper 16. pp. 365.
- Bjelm, L., S. Folin, and C Svensson. 1983. A radar in geological subsurface investigation. Bulletin of the International Association of Engineering Geology. 26-27:10-14.
- Collins, M. E., J. A. Doolittle, and R. V. Rourke. 1989. Mapping depth to bedrock on a glaciated landscape with ground-penetrating radar. Soil Sci. Soc. Am. J. 53: 1806-1812.
- Collins, M. E., W. E. Puckett, G. W. Schellentrager, and N. A. Yust. 1990. Using GPR for micro-analyses of soils and karst features on the Chiefland Limestone Plain in Florida. Geoderma 47:159-170.

- Collins, M. E., M. Crum, and P. Hanninen. 1994. Using ground-penetrating radar to investigate a subsurface karst landscape in north-central Florida. *Geoderma* 61:1-15.
- Daniels, D. J. 1996. *Surface-Penetrating Radar*. The Institute of Electrical Engineers, London, United Kingdom. 300 p.
- Daniels, D. J., D. J. Gunton, and H. F. Scott. 1988. Introduction to subsurface radar, *IEE Proceedings*, vol. 135F (4): 278-320.
- Davis, J. L. and A. P. Annan. 1989. Ground-penetrating radar for high-resolution mapping of soil and rock stratigraphy. *Geophysical Prospecting* 37: 531-551.
- Doolittle, J. A. 1987. Using ground-penetrating radar to increase the quality and efficiency of soil surveys. 11-32 pp. In: Reybold, W. U. and G. W. Peterson (eds.) *Soil Survey Techniques*, Soil Science Society of America. Special Publication No. 20. 98 p.
- Doolittle, J. A., R. A. Rebertus, G. B. Jordan, E. I. Swenson, and W. H. Taylor. 1988. Improving soil-landscape models by systematic sampling with ground-penetrating radar. *Soil Survey Horizons*. 29(2):46-54.
- Doolittle, J. A. and M. E. Collins. 1995. Use of soil information to determine application of ground-penetrating radar, *Journal of Applied Geophysics*, 33: 101-108.
- Holloway, A. L. and J. C. Mugford. 1990. Fracture characterization in granite using ground probing radar. *CIM Bulletin* 83(940):61-70.
- Jol, H. M., M. B. Junck and G. M. Kaminsky. 2000. High resolution ground penetrating radar imaging (225-900 MHz) of geomorphic and geologic settings: examples from Utah, Washington, and Wisconsin. 69-74 pp. IN: *Proceeding of the Eighth International Conference on Ground-Penetrating Radar*. David A. Noon, Glen F. Sticky, and Dennis Longstaff (editors). May 23 to 26, 2000, Goldcoast, Queensland, Australia. SPIE Vol. 4084. 908 p.
- Junck, M. B. and H. M. Jol. 2000. Three-dimensional investigation of geomorphic environments using ground-penetrating radar. 314-318 pp. IN: *Proceeding of the Eighth International Conference on Ground-Penetrating Radar*. David A. Noon, Glen F. Sticky, and Dennis Longstaff (editors). May 23 to 26, 2000, Goldcoast, Queensland, Australia. SPIE Vol. 4084. 908 p.
- Leggo, P. J., J. M. Glover, and M. R. Wajzer. 1992. The detection and mapping of kaolinitic clay by ground probing radar in the Cornish granites of southwest England. pp. 205-215. IN: P. Hanninen and S. Autio (eds.) *Fourth International Conference on Ground-Penetrating Radar*. 7 to 12 June 1992. Rovaniemi, Finland. Geological Survey of Finland, Special Paper 16. pp. 365.
- Morey, R. M. 1974. Continuous subsurface profiling by impulse radar. p. 212-232. IN: *Proceedings, ASCE Engineering Foundation Conference on Subsurface Exploration for Underground Excavations and Heavy Construction*, held at Henniker, New Hampshire. Aug. 11-16, 1974.
- Olson, C. G. and J. A. Doolittle. 1985. Geophysical techniques for reconnaissance investigations of soils and surficial deposits in mountainous terrain. *Soil Sci. Soc. Am. J.* 49: 1490-1498.
- Puckett, W. E., M. E. Collins, and G. W. Schellentrager. 1990. Design of soil map units on a karst area in West Central Florida. *Soil Science Society of America J.* 54:1068-1073.
- Robillard, C. P. Nicolas, P. Armirat, M. Garipey, and F. Goupil. 1994. Shallow Bedrock profiling using GPR. p. 1167-1179. IN: *GPR 94. Proceedings of the Fifth International Conference on Ground Penetrating Radar*. 12 to 16 June 1994. Kitchener, Ontario, Canada. Waterloo Center for Groundwater Research. pp. 1294.
- Rubin, L. A. and J. C. Fowler. 1978. Ground-probing radar for delineation of rock features. *Engineering Geology* 12: 163-170.
- Schellentrager, G. W. and J. A. Doolittle. 1991. Systematic sampling using ground-penetrating radar to study regional variation of a soil map unit. Chapter 12. p. 199-214. IN: Mausbach, M. J., and L. P. Wilding (eds.). *Spatial Variabilities of Soils and Landforms*. Soil Science Society of America Special Publication No. 28. pp. 270.
- Sigurdsson, T. 1994. Application of GPR for geological mapping, exploration of industrial mineralization and sulphide deposits p. 941-955. IN: *GPR 94. Proceedings of the Fifth International Conference on Ground Penetrating Radar*. 12 to 16 June 1994. Kitchener, Ontario, Canada. Waterloo Center for Groundwater Research. pp. 1294.

Stevens, K. M., G. S. Lodha, A. L. Holloway, and N. M. Soonawala. 1995. The application of ground-penetrating radar for mapping fractures in plutonic rocks within the Whiteshell Research Area, Pinawa, Manitoba, Canada. *Journal of Applied Geophysics*. 33:125-141.

**Table 1**  
**Locations of GPR Traverses**

Site	Traverse	File	Starting Point		Ending Point	
			Easting	Northing	Easting	Northing
GPR1	1	File10	37.16600	-112.31659	37.16526	-112.31622
	2	File11	37.16526	-112.31622	37.16511	-112.31562
	3	File12	37.16595	-112.31591	37.16596	-112.31590
	4	File13	37.16651	-112.31608	37.16651	-112.31607
	5	File14	37.16686	-112.31609	37.16685	-112.31610
	6	File15	37.16687	-112.31606	37.16751	-112.31620
	7	File16	37.16750	-112.31617	37.16699	-112.31664
	8	File17	37.16698	-112.31666	37.16644	-112.31653
			File18			
		File19				
GPR2	9	File20	37.16458	-112.33237	37.16519	-112.33273
	10	File21	37.16519	-112.33273	37.16559	-112.33350
	11	File22	37.16558	-112.33351	37.16588	-112.33459
	12	File23	37.16588	-112.33459	37.16655	-112.33467
	13	File24	37.16655	-112.33468	37.16719	-112.33519
	14	File25				
	15	File26	37.16657	-112.33526	37.16612	-112.33512
	16	File27	37.16606	-112.33511	37.16548	-112.33474
	17	File28	37.16548	-112.33474	37.16495	-112.33439
	18	File29	37.16495	-112.33439	37.16440	-112.33393
GPR3	19	File30	37.16440	-112.33393	37.16402	-112.33339
	20	File31	37.16440	-112.32494	37.16487	-112.32453
	21	File32	37.16490	-112.32444	37.16531	-112.32348
	22	File33	37.16526	-112.32336	37.16542	-112.32438
GPR4	23	File34	37.16541	-112.32438	37.16543	-112.32488
	24	File35	37.16543	-112.32487	37.16477	-112.32514
	25	File36	37.15930	-112.31579	37.15865	-112.31609
	26	File37	37.15866	-112.31609	37.15810	-112.31614
	27	File38	37.15815	-112.31611	37.15814	-112.31543
	28	File39	37.15813	-112.31541	37.15866	-112.31522
	29	File40	37.15863	-112.31522	37.15915	-112.31463
	30	File41	37.15914	-112.31465	37.15977	-112.31456
GPR5	31	File42	37.15984	-112.31449	37.15979	-112.31539
	32	File43	37.14405	-112.27170	37.14457	-112.27137
	33	File44	37.14445	-112.27136	37.14464	-112.27069
	34	File45	37.14463	-112.27066	37.14479	-112.27018
	35	File46	37.14479	-112.27017	37.14481	-112.26967
	36	File47	37.14503	-112.26972	37.14504	-112.27028
	37	File48	37.14504	-112.27027	37.14494	-112.27064
	38	File49	37.14493	-112.27063	37.14472	-112.27141
GPR6	39	File50	37.18421	-112.21752	37.18359	-112.21764
	40	File51	37.18358	-112.21765	37.18307	-112.21782
	41	File52	37.18307	-112.21783	37.18290	-112.21711
	42	File53	37.18291	-112.21711	37.18335	-112.21662
	43	File54	37.18366	-112.21671	37.18424	-112.21705
GPR7	44	File55	37.22735	-112.19547	37.22687	-112.19498
	45	File56	37.22687	-112.19499	37.22622	-112.19481
	46	File57	37.22601	-112.19490	37.22636	-112.19571
GPR8	47	File58	37.22632	-112.19565	37.22692	-112.19557
	48	File59	37.30199	-112.07536	37.30145	-112.07541
	49	File60	37.30143	-112.07581	37.30179	-112.07647
	50	File61	37.30179	-112.07646	37.30191	-112.07766
	51	File62	37.30191	-112.07766	37.30222	-112.07835
	52	File63	37.30220	-112.07835	37.30244	-112.07761
GPR9	53	File64	37.30245	-112.07762	37.30238	-112.07677
	54	File65	37.30242	-112.07676	37.30204	-112.07567
	55	File66	37.28123	-112.09718	37.28170	-112.09797
	56	File67	37.28170	-112.09798	37.28214	-112.09873
	57	File68	37.28215	-112.09877	37.28269	-112.09961
	58	File69	37.28270	-112.09964	37.28293	-112.10017
	59	File70	37.28297	-112.10020	37.28279	-112.10072
	60	File71	37.28280	-112.10072	37.28262	-112.10137
	61	File72	37.28263	-112.10136	37.28247	-112.10212
	62	File73	37.28244	-112.10198	37.28226	-112.10116
	63	File74	37.28226	-112.10117	37.28206	-112.10043

**Table 1**  
(continued)  
**Locations of GPR Traverses**

Site	Traverse	File	Starting Point		Ending Point	
			Easting	Northing	Easting	Northing
	64	File75	37.28205	-112.10040	37.28173	-112.09969
	65	File76	37.28177	-112.09963	37.28159	-112.09887
	66	File77	37.28157	-112.09870	37.28106	-112.09818
	67	File78	37.28105	-112.09817	37.28092	-112.09746

**Table 2**  
**Comparison of Radar Interpreted and Observed Depths  
to Subsurface Features**

Interpreted	Measured	Difference	Feature
0.66	0.61	0.05	lamella
0.59	0.59	0.00	lamella
1.08	0.85	0.23	lamella
0.71	0.71	0.00	lamella
1.52	1.70	-0.18	lamella
0.97	0.97	0.00	r
1.53	1.56	-0.03	cos
1.87	1.82	0.05	r
0.61	0.53	0.08	cr
1.07	0.91	0.16	r
0.20	0.17	0.03	cr
0.82	0.95	-0.13	r
0.62	0.69	-0.07	r
0.56	0.45	0.11	cr
0.82	1.05	-0.23	cr
2.10	2.55	-0.45	r
0.56	0.75	-0.19	cr
0.92	1.08	-0.16	r
0.43	0.44	-0.01	tree root
0.72	0.69	0.03	r
0.71	0.79	-0.08	r
0.41	0.42	-0.01	cr
0.46	0.52	-0.06	cr

**Table 3**  
**Radar Interpreted Depths to Bedrock**  
(m)

<u>File10</u>	<u>File11</u>	<u>File12</u>	<u>File13</u>	<u>File14</u>	<u>File15</u>
0.5	0.8	2.4	3.6	1.5	2.0
1.0	1.0	1.3	3.2	1.9	2.9
0.7	0.5	1.1	4.0	1.5	0.8
1.0	1.1	0.7	3.8	1.9	1.0
0.9	0.7	0.7	3.4	1.1	0.8
1.4	0.7	0.3	3.1	0.9	
1.2	2.1	3.9	3.3		
2.1		0.8	3.4		
2.1		1.0	2.5		
0.7		0.8			
0.6		0.5			
		0.7			
		1.1			
		1.4			
		1.1			
<u>File16</u>	<u>File17</u>	<u>File18</u>	<u>File19</u>	<u>File20</u>	<u>File21</u>
0.4	0.9	0.7	1.5	1.4	1.6
0.7	0.6	0.6	0.5	1.5	2.0
0.6	0.5	1.4	0.4	1.6	1.5
0.8	0.7	0.8	0.6	1.4	1.7
		0.3	0.6	1.0	1.7
		0.7		1.3	1.2
		0.6		1.2	1.3
		0.6		1.6	1.4
		1.2		1.3	1.5
				2.1	1.5
					1.6
					1.4
					1.4
<u>File22</u>	<u>File23</u>	<u>File24</u>	<u>File25</u>	<u>File26</u>	<u>File27</u>
1.2	1.2	0.8	0.8	0.8	1.8
1.4	1.5	0.7	0.5	0.7	0.7
1.6	1.4	1.0	0.5	1.1	0.8
1.1	1.4	0.6	0.8	0.9	1.3
1.6	1.4	0.6	0.5	0.8	1.3
1.5	1.4	0.6	0.5	1.1	1.1
1.5	1.5	0.9	0.6	1.6	0.8
1.4	1.5	0.5	0.7	1.3	0.8
1.6	1.6	0.7	0.4	1.3	1.2
1.5	1.2	0.9	0.4	1.6	
1.8					

**Table 3**  
**Radar Interpreted Depths to Bedrock**  
(m)

<u>File28</u>	<u>File29</u>	<u>File30</u>	<u>File31</u>	<u>File32</u>	<u>File33</u>
0.5	1.3	1.5	1.7	1.7	1.2
1.5	1.3	2.1	1.5	0.6	1.9
1.6	1.4	1.8	1.5	0.4	1.6
1.2	1.9	1.5	1.6	0.7	0.7
1.3	2.1	1.7	1.9	0.7	0.8
1.1	1.7	3.2	1.6	1.0	0.5
1.5	1.9	3.3	1.8	0.8	0.8
1.4	1.8	2.2	3.4	0.9	0.8
1.7	1.6		3.6	1.2	0.9
1.7	1.7		1.5	1.0	1.0
	1.8			1.1	

<u>File34</u>	<u>File35</u>	<u>File36</u>	<u>File37</u>	<u>File38</u>	<u>File39</u>
1.2	1.5	4.1	3.7	2.2	0.6
1.0	1.2	3.2	3.8	4.1	0.6
1.4	1.2	3.1	3.7	4.1	0.3
1.1	1.1	4.1	3.3	4.1	0.7
1.3	1.1	3.3	4.1	2.9	0.3
1.9	0.9	3.8	4.1	0.8	0.3
1.7	1.1	4.1	4.1	1.5	0.3
1.5	1.5	4.1	4.1	1.7	0.6
1.3	1.3	4.1	4.1	1.3	0.5
1.7	1.6	4.1	4.1	0.9	
		3.1			

<u>File40</u>	<u>File41</u>	<u>File42</u>	<u>File43</u>	<u>File44</u>	<u>File45</u>
0.5	1.1	0.4	0.7	1.0	0.8
0.3	0.4	0.4	0.5	0.7	2.2
0.7	0.8	1.0	0.6	2.0	2.1
0.9	0.5	1.2	0.3	2.1	1.9
0.8	0.9	1.3	1.0	1.9	0.7
0.8	0.8	1.0	1.1	2.2	0.2
0.5	0.4	1.0	0.7	2.1	0.4
0.7	1.1	0.6	0.8	2.1	0.3
0.5	1.6	1.1	0.8	1.2	0.6
0.5	1.8	0.5	0.9	1.2	0.5
		0.7			

<u>File46</u>	<u>File47</u>	<u>File48</u>	<u>File49</u>	<u>File50</u>	<u>File51</u>
0.7	0.8	0.8	0.8	1.0	0.8
0.4	0.4	1.1	0.7	0.8	0.7
0.3	0.7	1.0	1.4	0.8	0.6
0.3	0.4	1.4	1.7	0.9	0.8
0.3	0.4	0.7	1.9	1.4	0.5
0.7	0.5	0.7	1.9	0.8	0.6
0.7	0.7	0.7	2.2	0.9	0.6
0.8	0.7		2.2	0.6	0.6
0.6	0.7		1.8	1.5	0.5
0.5	0.8		1.8	1.7	0.6

**Table 3**  
**Radar Interpreted Depths to Bedrock**  
(m)

<u>File52</u>	<u>File53</u>	<u>File54</u>	<u>File55</u>	<u>File56</u>	<u>File57</u>
1.0	1.0	0.8	0.8	0.5	1.6
0.9	1.0	0.5	0.8	0.6	1.4
1.1	0.9	0.6	1.0	1.0	0.7
1.5	0.7	0.8	1.7	1.2	0.5
1.7	0.8	0.7	1.0	1.4	1.4
1.4	0.7	0.8	1.2	1.2	1.6
1.1	1.1	0.5	1.0	1.4	1.6
1.1	1.0	0.7	0.6	1.6	1.0
1.0	0.8	0.9	0.9	1.4	0.7
1.0	1.2	0.6	0.8	1.5	0.8
			0.7		1.0

<u>File58</u>	<u>File59</u>	<u>File60</u>	<u>File61</u>	<u>File62</u>	<u>File63</u>
1.2	1.9	1.1	2.1	4.1	4.1
1.4	2.2	1.7	2.5	4.1	4.1
1.4	2.1	0.6	1.7	3.8	4.1
1.3	1.7	0.6	1.6	4.0	4.1
1.3	1.5	0.9	1.5	4.1	3.3
1.6	1.8	1.0	1.4	3.7	2.1
1.6	1.6	1.7	1.7	3.9	1.9
1.7	1.8	1.7	1.6	3.7	1.3
1.6	2.7	1.6	1.7	4.1	1.3
1.7	1.6	2.2	1.9	4.1	1.6
			1.7		1.5
			1.9		
			1.9		
			2.3		

<u>File64</u>	<u>File65</u>	<u>File66</u>	<u>File67</u>	<u>File68</u>	<u>File69</u>
2.1	1.1	0.5	0.6	0.3	0.8
2.2	1.4	0.7	0.4	0.5	0.6
1.9	1.4	0.7	0.3	0.7	0.6
1.6	1.7	0.7	0.6	1.6	0.4
1.1	1.6	0.7	0.8	2.5	0.4
0.8	1.4	1.3	0.7	3.4	0.4
1.0	1.3	0.3	0.3	2.1	0.8
0.5	0.8	0.3	0.3	2.5	0.3
0.5	0.7	0.3	0.3	2.2	0.3
0.6	0.5	0.4	0.4	1.7	0.4
	0.5			1.1	
	0.6				
	0.8				

**Table 3**  
**Radar Interpreted Depths to Bedrock**  
(m)

<b>File70</b>	<b>File71</b>	<b>File72</b>	<b>File73</b>	<b>File74</b>	<b>File75</b>
0.7	0.6	4.1	0.8	0.4	0.6
0.4	0.5	3.6	0.9	0.0	1.2
0.6	1.1	3.8	1.2	0.0	1.0
0.6	1.6	2.7	1.5	0.4	1.5
1.4	1.6	2.1	1.9	0.5	2.4
1.2	2.0	2.1	1.7	0.6	1.8
0.8	2.4	1.5	0.8	0.5	1.4
0.5	2.3	0.9	0.8	0.6	1.3
0.3	3.7	0.4	0.6	1.1	1.8
0.5	4.1	0.6		0.5	2.0

<b>File76</b>	<b>File77</b>	<b>File78</b>
1.3	1.7	3.3
1.4	2.1	2.5
0.8	2.1	1.7
0.8	1.6	0.4
0.6	1.8	0.5
0.3	2.0	0.4
0.5	1.7	0.4
2.1	1.6	0.4
0.5	1.7	0.7
0.3	1.8	0.7

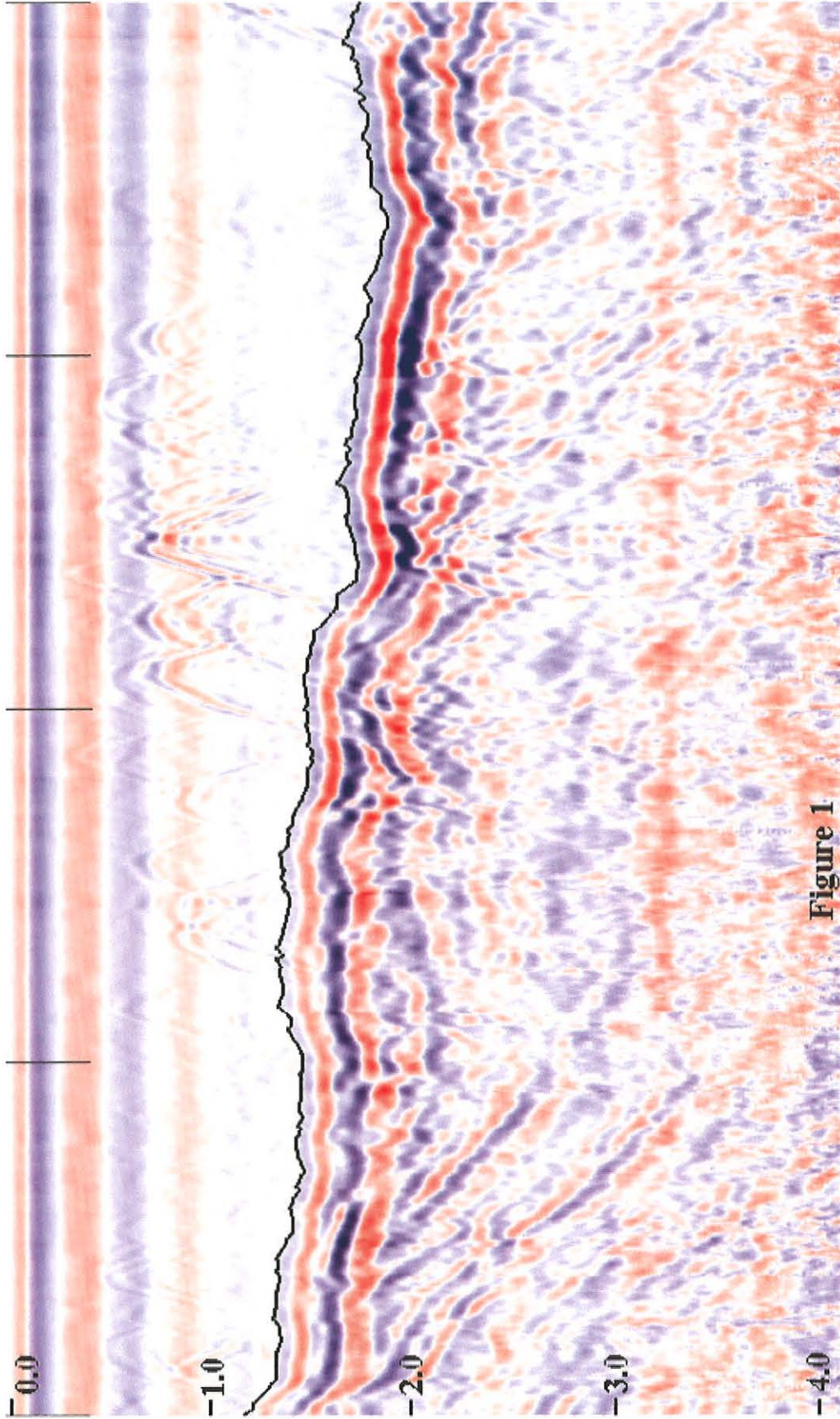
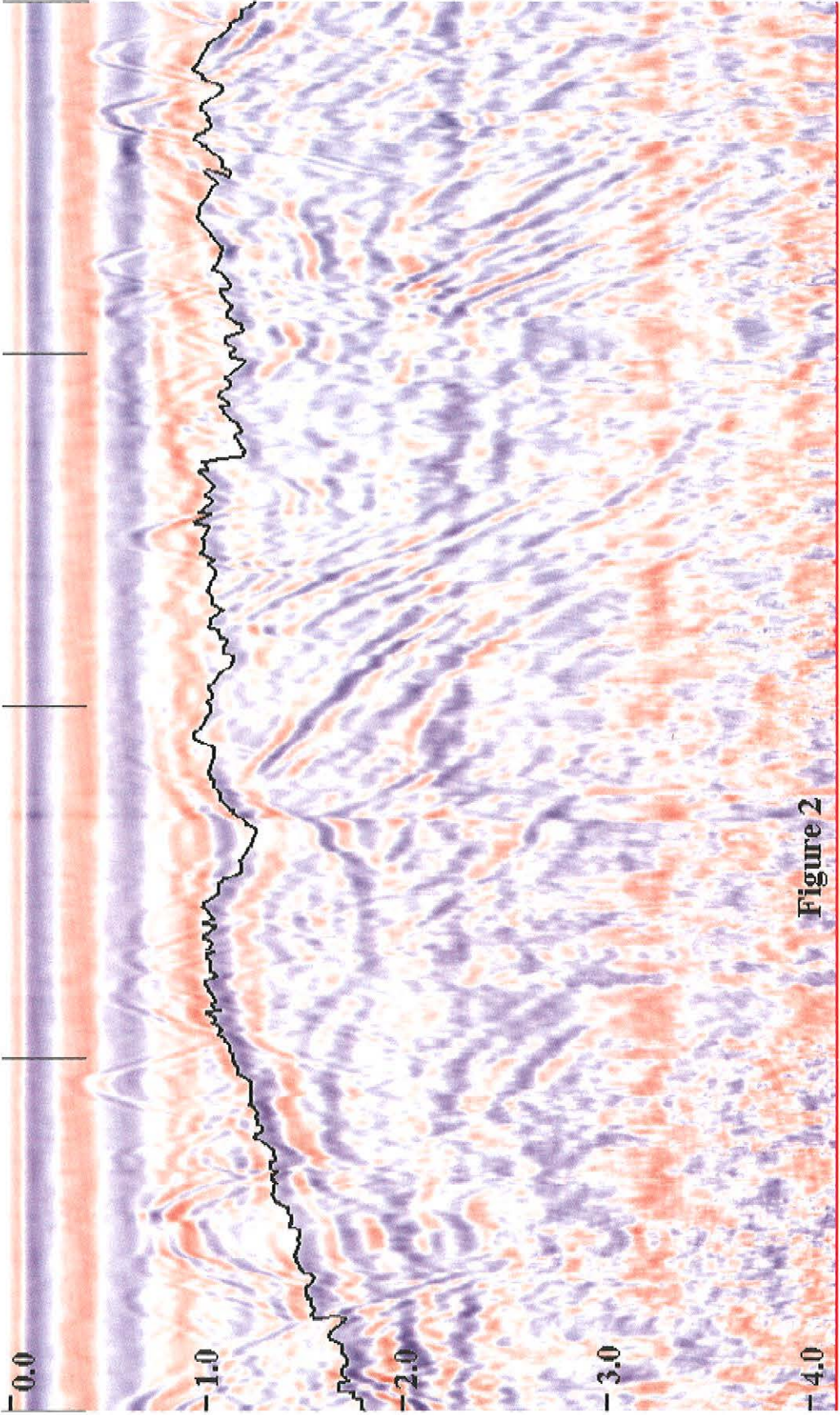


Figure 1



**Figure 2**

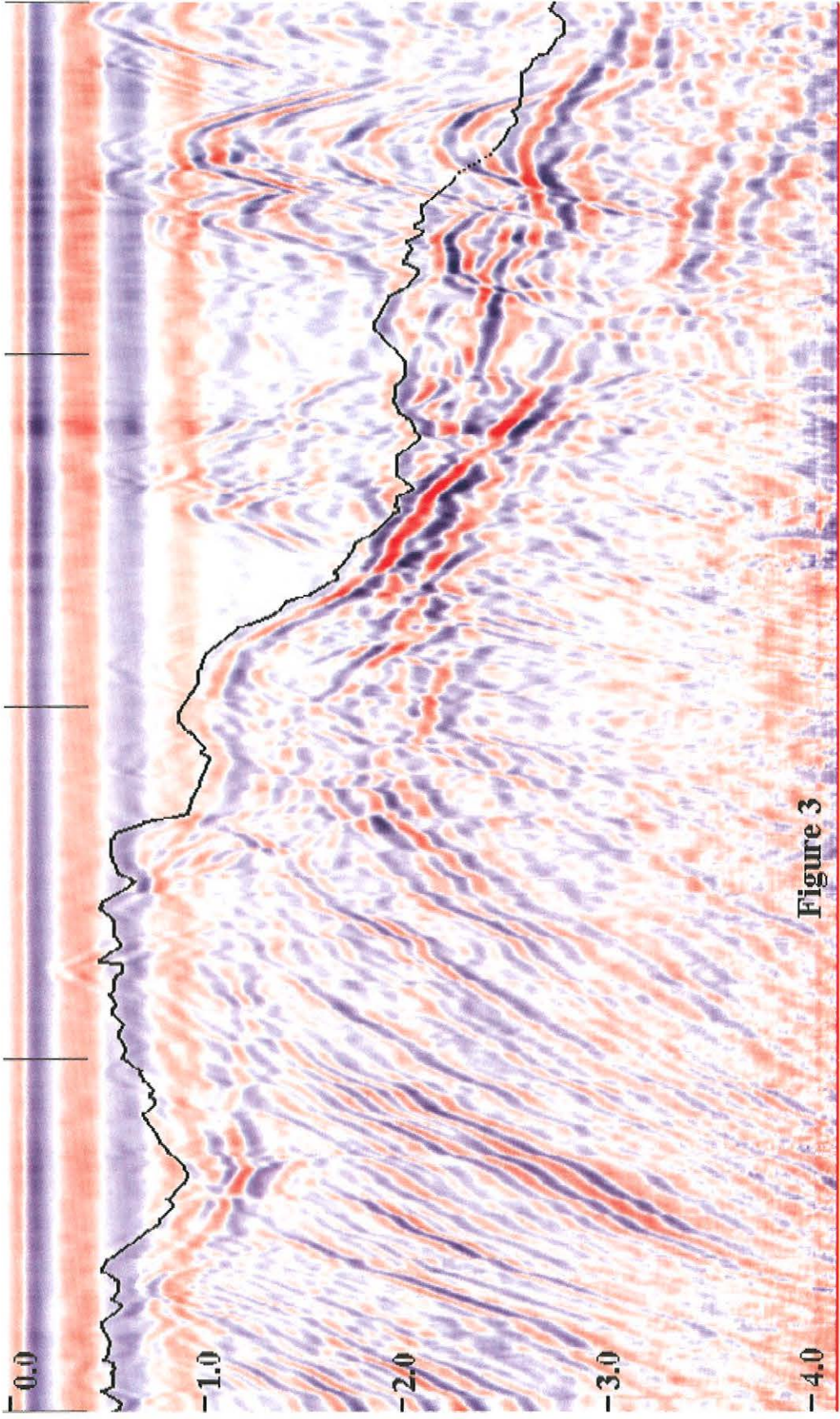


Figure 3